Aqueous Extract of Creosote Bush (*Larrea tridentata*) Leaves as Green Inhibitor for Carbon Steel in Hydrochloric Acid Solution

Ramses García Inzunza[1], Benjamín Valdez Salas[1,], Michael Schorr Wiener[1], Mónica Carrillo Beltran[1], Roumen Zlatev Koytchev[1], Margarita Stoytcheva Stilianova[1], Rogelio Ramos Irigoyen[1], Lidia Vargas Osuna[2], Juan Terrazas Gaynor[2],*

[1]Laboratorio de Corrosión y Materiales, Instituto de Ingenieria, Universidad Autonoma de Baja California,
Boulevard Benito Juárez y Calle de la Normal S/N, 21280 Mexicali, BC, México.
[2]Universidad Politecnica de Baja California, Calle de la Claridad S/N, Col. Elias Calles, Mexicali, BC, México.
[*]E-mail: benval@uabc.edu.mx

The inhibition of carbon steel corrosion in hydrochloric acid solution by the aqueous extract leaves of *Larrea tridentate* (AELL), a plant of Baja California, Mexico, has been studied by weight loss and potentiodynamic polarization techniques. The effect of temperature and immersion time of carbon steel (CS) in 1 M HCl with addition of extract, was studied too. It was also shown that the higher aqueous extract added, the higher corrosion inhibition was found. The thermodynamic adsorption parameters are shown in order to demonstrate the spontaneous adsorption; metallographic analysis results are also presented. The inhibition of AELL was performed via adsorption of the extract species on the CS surface. Potentiodynamic polarization results indicate that the aqueous extract acts as a mixed type corrosion inhibitor. The aqueous extract of Creosote Bush was analyzed by FTIR spectroscopy and phytochemical analysis. The results obtained confirm that the leaves extract of *Larrea tridentata* could serve as an efficient corrosion inhibitor for CS in hydrochloric acid media.

1. INTRODUCTION

The use of corrosion inhibitors is a quite popular method for corrosion prevention and control. Pickling acid is an accepted treatment of a metallic surface to remove contaminants, stains and steel rust using acid solutions, such as HCl and sulphuric acid (H_2SO_4), usually carried out at elevated temperatures. This treatment involves two main chemical reactions; dissolution of iron and hydrogen

evolution. In order to diminish the hydrogen evolution and the dissolution of iron, corrosion inhibitors are added to the corrosive media. [1] Recently, the use of plants and extracts in the field of corrosion science has increased widely and quickly. [2-3]. Sastri's volume belongs to the advanced field of "Green Chemistry" also known as sustainable chemistry, involving the design of chemical products and processes that reduce or eliminate the use or generation of hazardous substances. Green chemistry technologies provide a number of benefits: depresses waste, safer products, saving resources and energy, improved chemical manufacture and more. [4]

Creosote Bush is a perennial shrub from the Arizona and Sonoran Deserts. Numerous studies have demonstrated its antifungal activity, antiviral and nematicidal effects [5-7]. Among the proposed medicinal properties of Creosote Bush; the most prominent is its antioxidant effects [8].

The aim of the present work was to study the inhibitive action of aqueous extract leaves of Creosote Bush in the corrosion of CS immersed in an aqueous solution of 1.0 M HCl at different temperatures up to 75 °C, by using weight loss and potentiodynamic polarization technique. Thermodynamic parameters for inhibitor adsorption on CS were estimated and interpreted from Langmuir isotherms.

To identify the composition of the aqueous extract FTIR spectroscopy and phytochemical analyses were carried out.

2. EXPERIMENTAL

2.1. Materials

The corrosion experiments were performed on CS AISI 1018 with the chemical composition: 0.15–0.20% C, 0.60–0.90% Mn, 0.04 (max) P, 0.05 (max) S and the remainder is Fe.

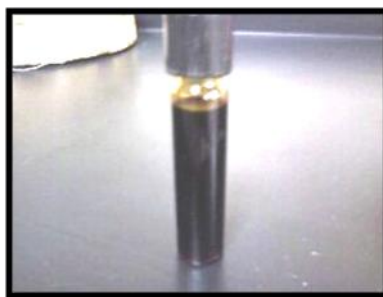### 2.2. Preparation of the aqueous extract (Stock solution)

Photo 1. Aqueous extract of *Larrea Tridentata* (Stock Solution).

The leaves of Creosote Bush were collected from the Sonoran Desert, located near Mexicali, Mexico. Dried plants were crushed into powder using a mortar. 100 grams of the powder were soaked in 2L of distilled water at 70°C for 30 minutes. The extract was filtered and almost all solvent was eliminated by azeotropic distillation of water at reduced pressure, prolonging the necessary distillation and/ or increasing depression as possible. The distillation yields a viscous and dark-brown extract which was the stock solution. (Photo 1).

The aqueous extract was characterized by Fourier Transform Infrared Spectroscopy; the FTIR spectrum was recorded using a PERKIN-ELMER100 FTIR spectrometer to determine the extract functional groups.

2.3. Phytochemical Screening.

Phytochemical screening for various compounds was carried out on the aqueous extract of the leaves of Creosote Bush [9].

2.4. Solutions

The stock solution was used to prepare solutions with different concentrations of inhibitor ranging from 0.1 to 1.5 gL^{-1} in 1M HCl solution which was prepared by dilution of analytical grade 37% HCl with distilled water.

2.5. Weight loss method

The CS coupons measuring 5 cm × 1.2 cm × 0.2 cm were polished with SiC paper from 100 to 600 grades and subsequently washed with methanol and then stored in a desiccator [10]. They were provided with a hole with uniform diameter to facilitate the suspension of the coupons in the test solution during the weight loss test. Accurate weight of the samples was obtained using an electronic balance METTLER TOLEDO.

The polished and CS coupons with uniform size were tied with threads and suspended in 50mL test solutions (in duplicate), with and without the inhibitor for different time intervals. The coupons were washed, dried, and weighed after the test; then the weight loss was calculated.

Exposure time and inhibitor concentrations used are:

- Time: 1, 3, 6, 24, 48, 120 h.
- Inhibitor concentration: 1.0, 1.5 gL^{-1}.

A constant temperature bath was used with a microprocessor temperature control (Koehler INSTRUMENT COMPANY, INC) to study the effect of temperature at different inhibitor concentrations, according to the following parameters:

- Inhibitor concentrations: 1.5, 1.0, 0.5, 0.1 gL^{-1}.
- Temperature: 75, 60, 40, 25 °C
- Time: 3 h

The corrosion rates (cr) of CS 1018 samples were determined according to the weight loss as a function of time.

$$cr = \frac{m1-m2}{At} \ , \tag{1}$$

where, m_1 and m_2 are the weights before and after corrosion. *A* is the total area of the coupon and *t* the corrosion time. From this data, inhibition efficiency (IE) was calculated by equation (2).

$$IE\ (\%) = \left(\frac{cr°-cr}{cr°}\right) \times 100, \tag{2}$$

where, cr° is the corrosion rate without inhibitor, cr is the corrosion rate with inhibitor.

2.6. Polarization measurements

The electrochemical analysis was performed using a three electrode system. The CS working electrode, saturated calomel reference electrode (SCE), and high purity graphite as counter electrode were used in the corrosion cell. Measurements were performed applying a Gamry Instrument Potentiostat/Galvanostat ZRA PC 4 and EIS CMS300 and DC CMS105 Corrosion Techniques software.

The working electrode was finished to 600 grit SiC paper, washed with methanol, and dried.

The polarization plots were obtained 10 minutes after the working electrode was immersed in the solution at 25°C using the Tafel Technique from −250mV to +250mV vs. corrosion potential (E_{corr}) at 1mV/s scan rate.

The inhibition efficiency was calculated following equation 3. [11]

$$IE\ (\%) = \left(\frac{i°corr-icorr}{i°corr}\right) \times 100, \tag{3}$$

where, $i°_{corr}$ is corrosion current density without inhibitor. i_{corr} is corrosion current density with inhibitor.

The gravimetric and electrochemical corrosion tests were conducted in accordance with the practices recommended in ASTM standards G3, G5, G31 [12, 13, 14].

2.7. Micrographs

A Metallographic Microscope (MARK V Laboratory, Metallographics Equipment & Supplies) was utilized to view the surface of the CS coupons before and after immersion in HCl. The representative ones are presented.

3. RESULTS AND DISCUSSION

3.1. Weight loss method.

The weight loss results for CR showed that the aqueous extract of Creosote Bush decreases the corrosion rate when the immersion time increases, (Table 1).

The inhibition efficiency of 1.5gL^{-1} concentration is higher than 1.0 gL^{-1} at immersion times of 1 to 6 hours; however, from 24 to 120 hours, the inhibition efficiency at 1.5 gL^{-1} and 1.0 g L^{-1} are alike. This indicate that the higher concentration of the aqueous extract is added, the faster adsorption will be on the metal surface, nevertheless, after the 24 hours test, the adsorption coverage for 1.5 gL^{-1} and 1.0 gL^{-1} is the same. The highest efficiency (88.27%) was obtained with the 1.0 gL^{-1} of inhibitor concentration after 120 hr of testing. While 1.5gL^{-1} was 87.93%. Inhibition efficiencies are shown in Table 2.

Table 1. Corrosion rates with and without Creosote Bush aqueous extract.

Inhibitor concentration, gL^{-1}	Immersion time, h Corrosion rate, mg·cm^{-2}·h^{-1}					
	1	3	6	24	48	120
Blank	0.5416	0.4722	0.4225	0.3470	0.3031	.2645
1.5	0.2000	0.0847	0.0756	0.0486	0.0369	0.032
1.0	0.2696	0.1197	0.1021	0.0433	0.0367	0.031

Table 2. Inhibition efficiency of Creosote Bush aqueous extract

Inhibitor concentration, gL^{-1}	Immersion time, h Inhibition Efficiency, %					
	1	3	6	24	48	120
Blank	-	-	-	-	-	-
1.5	63.07	80.81	82.10	86.57	87.82	87.93
1.0	50.22	74.65	75.83	87.52	87.89	88.27

3.2. Polarization Measurements

The effect of the inhibitor concentration on the electrochemical polarization curves is for CS 1018 in 1M HCl solution at room temperature with EALL (Figure 1). The electrochemical corrosion parameters: current density (icorr), cathodic and anodic Tafel slopes (βc and βa), and the percentage efficiency (IE) at different concentrations of the plant extract are given in Table 3.
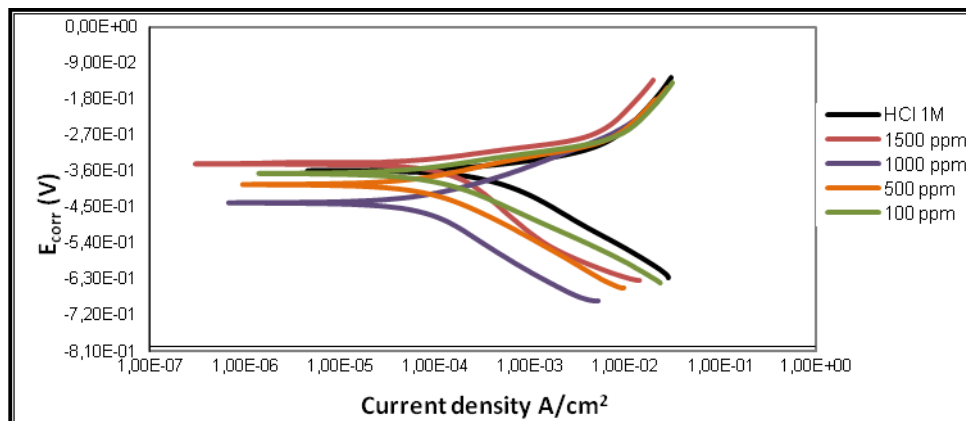

Figure 1. Anodic and cathodic plots of carbon steel 1018 in 1M HCl solution in the absence and presence of various concentrations of Creosote Bush aqueous extract.

Table 3. Polarization parameters for carbon steel in 1M HCl at room temperature containing various concentrations of Creosote Bush aqueous extract.

Concentration gL^{-1}	E_{corr} mV/SCE	β_c mV/dec	B_a mV/dec	i_{corr} $\mu A/cm^2$	IE %
Blank	-358.0	163.1	119.3	583.0	-
0.1	-366.0	119.1	85.4	127.0	78.21
0.5	-392.0	139.4	91.10	111.0	80.96
1.0	-439.0	171.0	91.50	96.60	83.43
1.5	-341.0	146.5	78.80	75.60	87.03

Polarization studies revealed that the corrosion current density (i_{corr}) decreased noticeably with the addition of the extract. Further, there was an anodic shift of the E_{corr} value from -358mV (blank) to -341mV at 1.5 gL^{-1} indicating that the Creosote Bush leaves extracts acted as an anodic inhibitor [15] for CS 1018 in 1M HCl, which was supported by the gradual and significant decrease of the anodic Tafel slope, β_a from 119.3mV/decade in the blank to 78.80mV/decade in 1.5 gL^{-1}. At lower solution inhibitor concentrations, the values of the cathodic Tafel slopes were decreasing too, though not

markedly. This means that the extract must have acts by blocking both anodic and cathodic sites, as a mixed type of inhibition.

3.3. Effect of temperature.

Table 4 shows the corrosion rates at different temperatures for Creosote Bush aqueous extract in the concentrations studied for 3 hours of immersion.

Table 4. Corrosion rates for carbon steel in 1M HCl at different temperatures and concentrations of Creosote Bush aqueous extract.

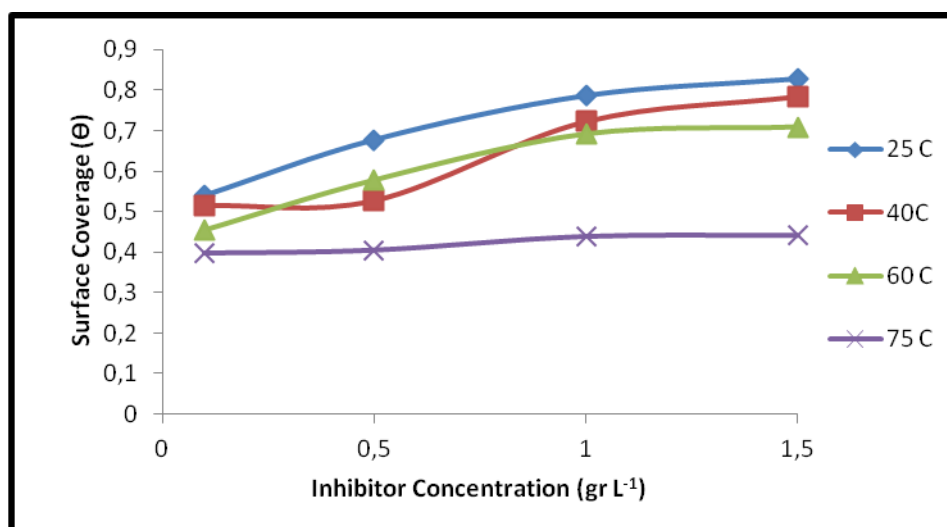| Inhibitor Concentration, gL^{-1}	Temperature, °C Corrosion rate, mg·cm^{-2}·h^{-1}			
	25	40	60	75
Blank	0.4447	0.6864	3.8513	28.7876
1.5	0.0769	0.1473	1.1187	16.0714
1.0	0.0952	0.1895	1.1849	16.1324
0.5	0.1435	0.3238	1.6247	17.1152
0.1	0.2045	0.3322	2.1003	17.3356

Figure 2. Variation of surface coverage with extract concentration for carbon steel in 1 M HCl at different temperatures.

It is clear that the rise in temperature increases the corrosion rate of CS, and adding up the aqueous extract reduce the corrosion rate under the parameters studied.

Figure 2 presents the effect of temperature under different concentrations of the aqueous extract of Creosote Bush. The IE is decreasing when the temperature is increasing due to desorption of corrosion inhibitor from the metal surface. A relatively small increase in the IE is observed with rise in temperature to 60 °C for CS corrosion at 0.5 gL^{-1} of the aqueous extract in 1M HCl.

3.4. Adsorption isotherms.

The primary step in the mechanism of action of the inhibitors in acid solutions is generally its adsorption on the metal surface, which is usually oxide free in acid solutions. Bockris [16] states that the adsorption of an organic substance onto the metal surface can be expressed by the following exchanger reaction:

$$Org_{(sol)} + nH2O_{(ads)} \Longleftrightarrow Org_{(ads)} + nH2O_{(sol)}, \qquad (4)$$
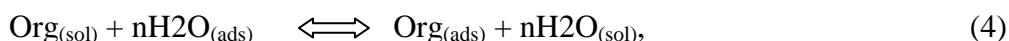
where n is the number of water molecules displaced of the metal surface by one molecule of the adsorbed inhibitor; the value of n depends on the transversal section of the organic molecule area with respect to the water molecule. The adsorption of the organic molecules occurs because of the interaction between the energy on the metal surface and the inhibitor is greater than the interaction of the energy on the metal surface and the water molecules. When the equilibrium of the process described in (4) is reached, it is possible to obtain diverse expressions of the adsorption isotherm plots, and thus, the degree of surface coverage (θ = IE(%)/100) can be plotted as a function of the inhibitor concentration under test.

Figure 2 demonstrates that θ increases with the inhibitor concentration; this is attributed to more adsorption of inhibitor molecules onto the CS surface. The surface coverage values (θ) for different concentrations of the inhibitor in an acid medium have been evaluated from the corrosion rate data. The data were plotted to obtain a suitable adsorption isotherm (Figure 3).The Langmuir adsorption isotherm [17] was applied to analyze its mechanism by the following:

$$\frac{C}{\theta} = \frac{1}{K} + C \qquad (5)$$

where C is the inhibitor concentration in mL L^{-1} in the electrolyte, and $K_{e.c.a}$ (mL^{-1} L) is the equilibrium constant for the adsorption/desorption process.

The estimated adsorption parameters from Langmuir adsorption isotherms are given in Table 5. It indicates that the inhibitor obeys the Langmuir model since that the experimental data presents adequate curve fittings for the applied adsorption isotherms; the correlation coefficients (r^2) were in the range: $0.9997 \geq r^2 \geq 0.9882$ for temperatures of 25 to 60 °C, at 75 °C the slope is 2.2, contrary, to what is expected for ideal Langmuir adsorption equation. That is explained because a rise in temperature induces reaction of the organic molecules having polar atoms or groups which are adsorbed on the

metal surface, which leads to a repulsion and attraction; this is the reason for the divergence of the slope value from unity.
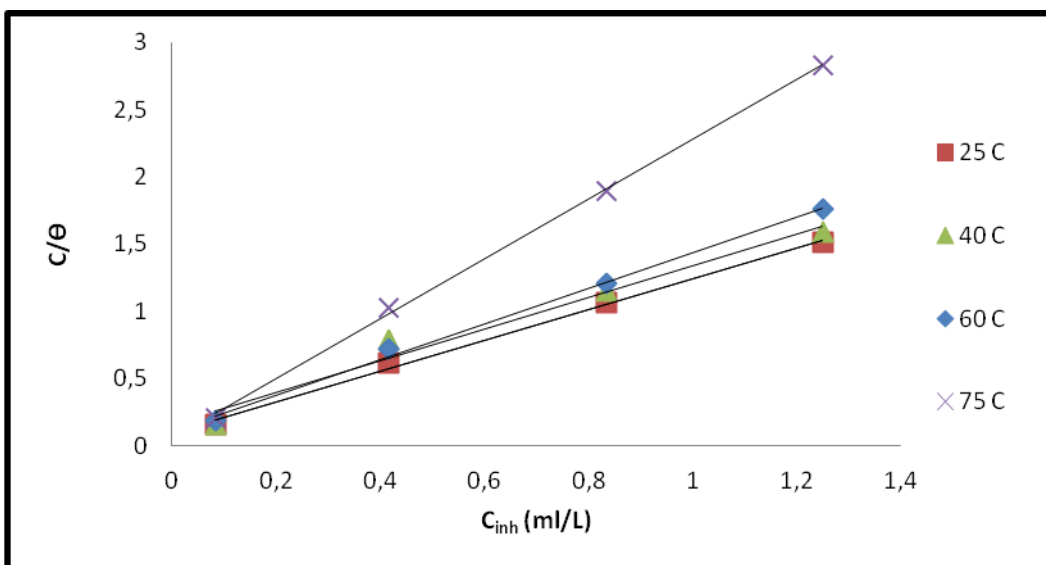

Figure 3. Langmuir adsorption isotherm of AELL on carbon steel 1018 surface in 1M HCl.

Table 5. Adsorption parameters for AELL in 1M HCl obtained from Langmuir adsorption isotherms at different temperatures.

Temperature, °C	Adsorption parameters		
	slope	K_{ads}, ml ^{1}L	r^2
25	1.14	10.76	0.9997
40	1.17	6.15	0.9882
60	1.32	9.14	0.9993
75	2.2	18.79	0.9996

3.5. Thermodynamic adsorption isotherms.

Thermodynamic adsorption data, such as change in free energy (ΔG_{ads}), adsorption heat (ΔH_{ads}), and the entropy of adsorption (ΔS_{ads}), can be calculated depending on the estimated values of K from adsorption isotherms [18] at different temperatures:

$$K_{ads} = .018\exp[-\Delta G_{ads}/(RT)] \qquad (6)$$

the ΔG_{ads} obtained values are plotted versus T (Figure 4) in accordance with the basic equation [19]:

$$\Delta G_{ads} = \Delta H_{ads} - T\Delta S_{ads}. \qquad (7)$$

A straight line of interception represents the ΔH_{ads} values. By introducing the values in (7), the ΔS_{ads} values are calculated at all studied temperatures. As it can be observed in Figure 4, a segmented straight line of two opposite slopes was obtained in 1M HCl indicating the existence of two sets of adsorption sites with different energetic enthalpies of adsorption, leading to the occurrence of a comprehensive adsorption. The negative values of ΔG_{ads} indicate that the adsorption of AELL on the CS 1018 surface is a spontaneous process [20-21]. Usually the adsorption free energy involved in a physisorption process is < 40 KJ/mol [22].
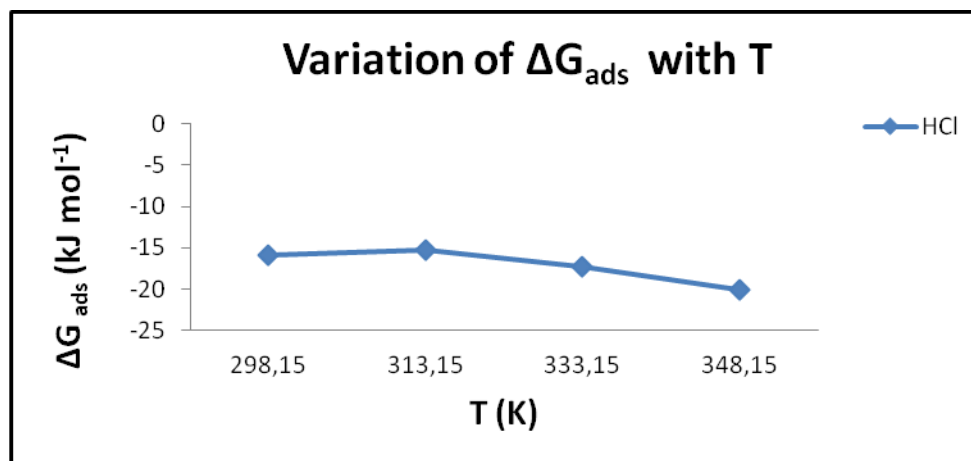

Figure 4. The variation of ΔG_{ads} with temperature

ΔG_{ads} value decreases (becomes more negative) with rise in temperature. The most negative value of ΔG_{ads} (Table 5) occurs at 75°C. According to the value of ΔH_{ads}, (Table 6) the following results are obtained:

- In 1M HCl solutions, both endothermic ($\Delta H_{ads}= 28.513$ kJ mol^{-1}) and exothermic ($\Delta H_{ads}, =-28.5213$ kJ mol^{-1}) adsorption behavior were detected depending on the exact range of applied temperatures. The adsorption becomes endothermic at 40°C after have been an exothermic adsorption at 25°C. The absolute values of the heat of adsorption is larger than the common physical adsorption heat, but smaller than the common chemical adsorption heat [23]; it probably indicates that both physical and chemical adsorption took place on the surface of the metal in AELL-HCl system.

The positive values of ΔS_{ads} are accompanied with endothermic adsorption process, while negative ΔS_{ads} values are accompanied with exothermic adsorption process. This agrees with what expected, when the adsorption is an exothermic process, it must be accompanied by a decrease (becomes more negative) in the entropy change [24].

Table 6. Thermodynamic adsorption parameters for AELL on carbon steel 1018 in 1M HCl at different temperatures.

Temperature, °C	ΔG kJ mol^{-1}	ΔH, kJ mol^{-1}	ΔS, kJ mol^{-1}
25	-15.848	-28.968	-0.044
40	-15.188	28.513, - 28.968	-0.044, 0.1389
60	-17.258	28.513	0.1389
75	-20.120	28.513	0.1389

3.7 Photomicrographs

The micrographs are made before and after immersion of the test coupons in HCl at different temperatures, with and without the plant extract (Figures 5A to 5G). There was massive general corrosion of the CS in the test medium without AELL, (Figures 5B, D, and F).
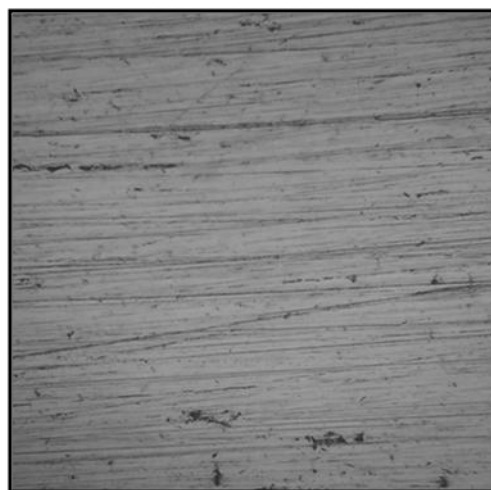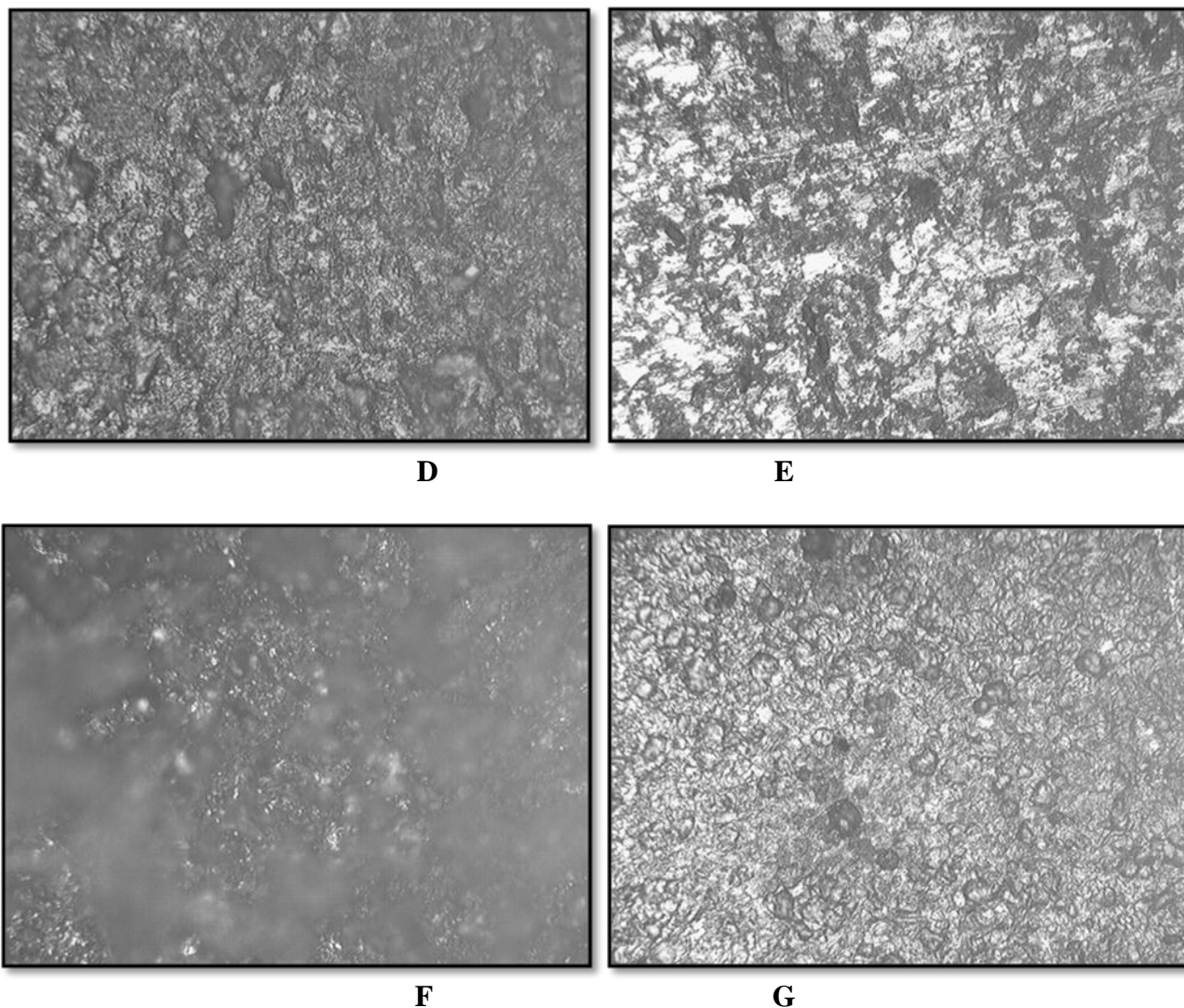
A
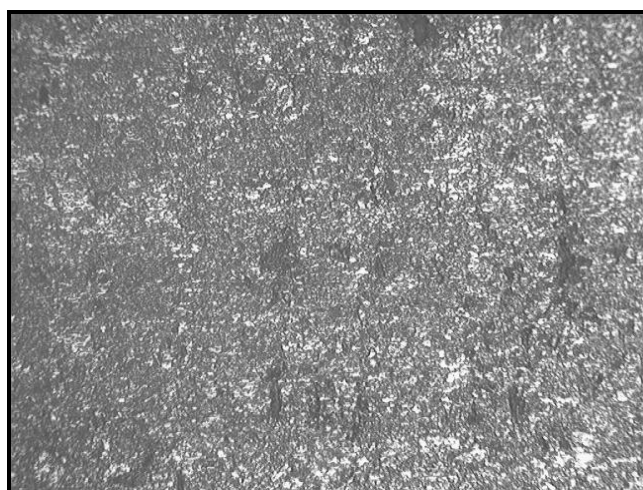
B
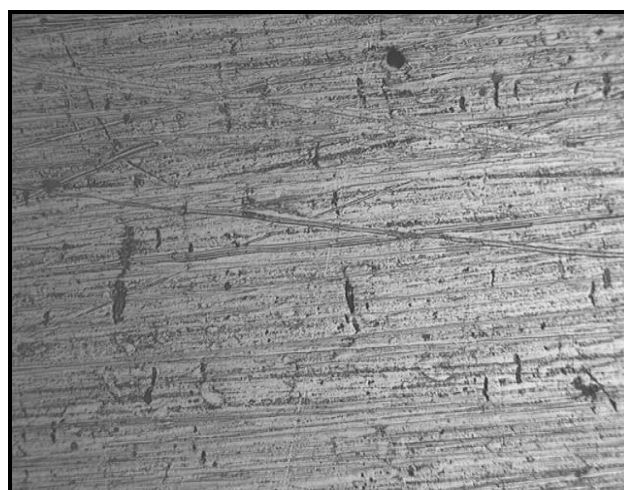
C

Figure 5. A) Test coupon before test immersion in hydrochloric acid. B) Test coupon after test immersion at 40 °C without AELL. C) Test coupon after test immersion with 1.5gL^{-1} at 40 °C. D) Test coupon after test immersion at 60 °C without AELL. E) Test coupon after test immersion with 1.5 g L^{-1} at 60°C. F) Test coupon after test immersion at 75 °C without AELL. G) Test coupon after test immersion with 1.5 g L^{-1} at 75°C.

Figure 5C shows good protection of the surface with the addition of 1.5 gL^{-1} of AELL in 1 M HCl at 40 °C. The figures 5E and 5G confirm our expectation, because the coupon test immersed in 1M HCl at 60°C with 1.5 gL^{-1} of AELL evidence better protection than the coupon immersed at 75 °C. These observations from the micrographs bear very close correlation with the results obtained from the weight loss method, the corresponding cr and inhibition efficiencies.

4. PHYTOCHEMICAL SCREENING.

Phytochemical screening was carried out on the AELL; it proofs the presence of the organic compounds. (Table 6).

Table 6. Phytochemical screening of AELL.

Phytochemical essay	Functional Groups	Presence
Dragendorff	Alkaloids	-
Liebermann-Burchard	Triterpens and/or steroids	+
Börntrager	Quinones	-
Hydroxylamine - iron(III) chloride	Lactones	+
Foam	Saponins	+
Ferric chloride	Phenol and/or tannin	+
Fehling	Reducing sugar	+
Shinoda	Flavonoid	+
Amines	Amines	+
Mucilage	Mucilage	+

Several articles record the presence of the different compounds in the leaves which are in good agreement to the phytochemical screening performed. Lignans dominate the leaves chemistry, especially nordihydroguaiaretic acid (NDGA), at 1.6–6.55% [25] and 15-20% of the dried leaves [26]; plus dihydroguaiaretic acid, mesodihydroguaiaretic acid, 3-methoxyisoguacin, 3'-demethoxyisoguaiacin [27, 28], 6,3'-di-O-demethylisoguaiacin (previously designated 3'-dydroxynorisoguaiacin), 6-O-demethylisoguaicin (norisoguaiacin), didehydro-3'-demethoxy-6-O-demethylguaiacin, 3'-demethoxy-6-O demethylguaiacin [29], 4-epi-larreatricin, larreatricin, 3',3"-dimethoxylarreatricin, 3,4-dehydrolarreatricin, larreatridenticin, 3,4-dehydrolarreatricin, larreatridenticin, and others [30]; flavonoids include 2,6-di-C-glucopyranosylapigenin, 6,8-di-C-glucopyranosylchrysoeriol, gossypetin 3,7-dimethyl ether, 5,8,4'-trihydroxy-3,7,3'-trymethoxyflavone[31], quercetin, kaempferol, rhamnetin, rutin [31]; saponins/triterpenes, including larreagenin A, larreic acid, erythrodiol-3-β-(4-hydroxy-cinnamdyl), erythrodiol-3-β-(4-dihydroxy cinnamdyl) [31,32].

4.1. Infrared Analysis.

The IR spectra (Figure 6) of the extract of *Larrea Tridentata* presents similarity with the IR spectra of a saponin [33] which contain bands corresponding: phenolic hydroxyl groups (3348.86 cm^{-1}); carbonyl group (1599.9 cm^{-1}), as well as, several bands between 1383.86 and 1041.63 cm^{-1} that are diagnostic for the spiroketal side chain [34].

Saponins/Triterpens are 10-15% approximately of the dry weight of *Larrea Tridentata* leaves [26]. The FTIR Spectroscopy is not capable to determine exactly the main compound of the present extract, but manifest what it is the more abundant chemical compound. Numerous compounds are in

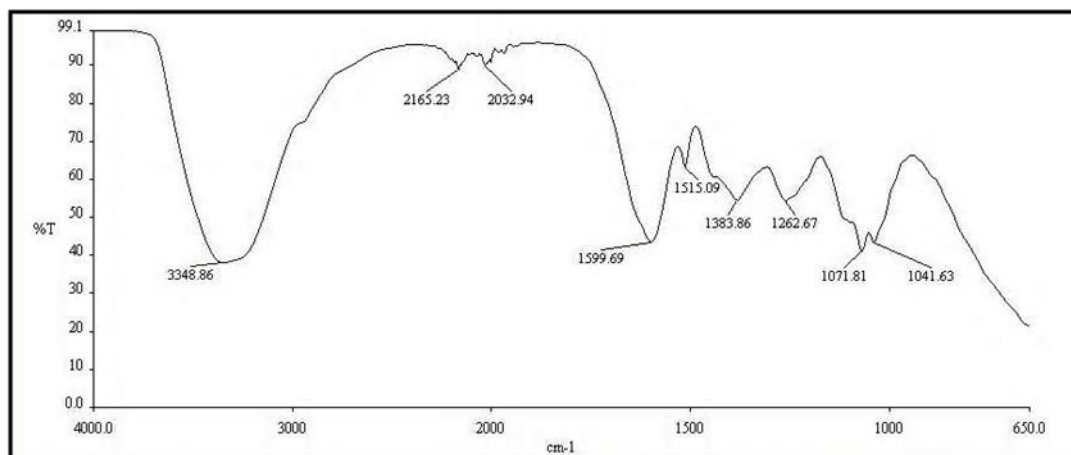the aqueous extract in lesser concentration, except for phenolic/lignans, according to several papers [26].

Figure 6. IR Spectra aqueous extract *of Larrea Tridentata.*

4.2 Mechanism of inhibition

The inhibition mechanism involves the adsorption of the inhibitor on the metal surface immersed in aqueous HCl solution. Four types of adsorption [35] may take place involving organic molecules at the metal–solution interface: electrostatic attraction between the charged molecules and the charged metal; interaction of unshared electron pairs in the molecule with the metal; interaction of π-electrons with the metal; and a combination of all the above.

The predominant adsorption mode depends upon factors such as the extract composition, type of acid anion, as well as chemical changes in the extract. There are two ways to explain the inhibition of the dissolution reaction by adsorption at the metal surface [36]. In acid solution, the protonation of the EALL may occur easily, so it is difficult for the protonated leaves extract to approach the positively charged carbon steel surface (H_3O^+/metal interface) due to the electrostatic repulsion. Since chloride ions have a smaller degree of hydration, thus they could bring excess negative charges in the vicinity of the interface and favour more adsorption of the positively charged inhibitor molecules, the protonated leaves extract adsorbed through electrostatic interactions between the positively charged molecules and the negatively charged metal surface. Another way to explain the inhibition involves the donation of lone pairs of electrons to the surface and the interaction of π-electrons of the aromatic/heterocyclic ring with the metal surface, which may be the main role. The two ways can influence in the inhibition corrosion in cooperative mode.

The compounds identified for diverse authors, as well as the phytochemical essays and FTIR analysis proved the presence of flavonoids, triterpens/saponins, amines, reducing sugar, phenol and tannins. Functional groups as C-O, N-H, O-H, C=O, O-heterocyclic rings in their molecular structures, as well as aromatic rings are contained in AELL. These functional groups have been reported in other literature as effective corrosion inhibitors [37-38].

4. CONCLUSIONS

The inhibition effect of AELL on CS in HCl solution was examined by weight loss methods and potentiodynamic polarization. The aqueous extract of *Larrea Tridentata* leaves showed significant corrosion inhibition activity. The inhibition efficiency value increases with the increasing of inhibitor concentration. Polarization curves indicated that AELL acts as a mixed type inhibitor in 1 M HCl. The inhibition is accomplished by adsorption of the extract components on the steel surface; the adsorption is spontaneous and obeys the Langmuir isotherm. Micrographs offer a perfect proof for the formation of a protective layer of green inhibitor over the CS surface, thus preventing corrosion. The organic molecules, such as lignans, flavonoids and amines but mainly saponins present in AELL are responsible for the corrosion inhibition effect.

References

1. H. H. Uhlig, *Corrosión y control de corrosión,* Urmo, Bilbao (1979).
2. P. B. Raja and M. G. Sethuraman, *Materials Letters*, 62 (2008) 113–116.
3. R. Garcia Inzunza, B. Valdez Salas, R. Kharshan, A. Furman and M. Schorr Wienner, *International Journal of Corrosion*, Article ID 980654 (2012), 8 pages.
4. V.S. Sastri, *Green Corrosion Inhibitors,* Wiley, New Jersey (2011).
5. R. H. Lira Saldivar 21 (2003) 214-22.
6. S. Moreno-Limón, L.N. González-Solís, S.M. Salcedo-Martínez, M.L. Cárdenas-Ávila y A. Perales-Ramírez, *Polibotánica*, 32 (2011) 193-205.
7. Severine Van Slambrouck, Amber L. Daniels, Carla J. Hooten, Steven L. Brock, Aaron R. Jenkins, Marcia A. Ogasawara, Joann M. Baker, Glen Adkins, Eerik M. Elias, Vincent J. Agustin, Sarah R. Constantine, Michael J. Pullin, Scott T. Shors, Alexander Kornienko Wim F.A. Steelant *Oncology Reports* 17 (2007) 1487-1492.
8. Sheikh, N., Philen, R., Love, L.,. *Archives of International Medicine* 157 (1997) 913–919.
9. A. Lourenço, L. Cruz López, and A. San Feliciano, *Extracción, Fraccionamiento y Aislamiento de Compuestos Activos,* Programa Iberoamericano de Ciencia y Tecnología para el desarrollo, España (2010).
10. A. Y. El-Etre and Z. El-Tantawy, *Portugaliae Electrochimica Acta*, 24 (2006) 347–356.
11. M. Scendo, *Corrosion Science*, 5 (2008) 1584–1592.
12. ASTM G3-89, "Standard Practice for Conventions Applicable to Electrochemical Measurements in Corrosion Testing," 2010.
13. ASTM G5-94, "Standard Reference Test Method for Making Potentiostatic and Potentiodynamic Anodic Polarization Measurements," 20011.
14. ASTM G31-72, "Standard Practice for Laboratory Immersion Corrosion Testing of Metals," 2004.
15. O. L. Riggs Jr., *Corrosion Inhibitors*, Edited by C. C. Nathan, NACE, Houston, 1973.
16. J. O. M. Bockris and D. A. J Swinkels, *Journal of The Electrochemical Society*, 111 (1964) 735.
17. I. Langmuir, *Journal of the American Chemical Society*, 39 (1947) 1848.
18. E. A.Noor, *International Journal of Electrochemical Science*, 2 (2007) 996–1017.
19. A. A. El-Awady, B. A. Abd-El-Nabey, and S. G. Aziz, *Journal of the Electrochemical Society*, 139 (1992) 2149–2154.
20. M. Elachouri, M. S. Hajji, M. Salem et al., *Corrosion*, 52 (1996) 103–108.
21. B. V. Savithri and S. M. Mayanna, *Indian Journal of Chemical Technology*, 3 (1996) 256–258.
22. Eddy N.O, and S.A. Odoemelam, *J.Surface Sci. Technol.,* 24 (2008) 1-14.
23. G. Mu, X. Li, and G. Liu, *Corrosion Science*, 47 (2005) 1932– 1952.

24. Ronald J. Gillespie, Aurelio Leltrán, *Quimica,* Reverté, Barcelona, 1990.
25. J. L. Valentine et al., *Anal Lett.,* 17 (1984) 1617
26. Brinker. F *British Journal of Phytotherapy* 3 (1993) 10-30.
27. F.R.Fronczeketal., *J.Nat.Prod.,* 40 (1987) 497
28. O. Gisvold and E. Thaker, *J. Pharm. Sci.*, 63, (1974) 1905
29. C. Konno et al., *J. Nat. Prod.*, 52 (1989) 1113
30. C. Konno et al., *J. Nat. Prod.*, 53 (1990) 396
31. M. Sakakibrara et al., *Phytochemistry,* 15 (1976) 727.
32. Mabry, T.J., J.H. Hunziker, D.R. Difeo Jr. "*Creosote Bush: Biology and Chemistry of Larrea in New World Deserts"* Dowden Hutchinson & Ross, Inc, Stroudsburg (1977).
33. http://riodb01.ibase.aist.go.jp/sdbs/cgi-bin/direct_frame_top.cgi, (2013)
34. Edward S. Rothman, Monroe E. Wall , C. Roland Eddy, *J. Am. Chem. Soc.*, 74 (1952) 4013–4016.
35. D. P. Schweinsberg, A. Graeme, George, A. K. Nanayakkara and D. A. Steinert, *Corros. Sci.* 28 (1988) 33.
36. F. Bentiss, M. Traisnel and M. Lagrenee, *J. Appl. Electrochem.,* 31 (2001) 41.
37. M. Shyamala and P. K. Kasthuri, *International Journal of Corrosion*, Article ID 852827 (2012) 13.
38. I. E. Uwah, P. C. Okafor, and V. E. Ebiekpe, *Arabian Journal of Chemistry*, 10 (2010) 008.